Capacity Credit Assessment of Cyber Physical Power System Considering Climate Change

Bo Li *
School of Electrical Engineering
Guangxi University
Nanning, China
boli@gxu.edu.cn
*Corresponding author

Zhipeng Huang
School of Electrical Engineering
Guangxi university
Nanning, China
2312392040@st.gxu.edu.cn

2025 IEEE International Conference on Power Systems and Smart Grid Technologies (PSSGT) | 979-8-3315-1140-1/25/$31.00 ©2025 IEEE | DOI: 10.1109/PSSGT64932.2025.11034279

***Abstract*—The cyber-physical power systems (CPPS) are highly coupled with the physical power systems and the information systems. Therefore, the reliability evaluation of the CPPS needs to consider the impact of cyber-attacks or communication failures. Climate-induced temperature increases have an effect on both load demand and energy supply systems, which can lead to a drop in power system reliability. Thus, this paper presents a capacity credit assessment framework to evaluate the effect of climate change and multiple storage technologies on cyber-physical power system adequacy. First, the effects of information system failures on physical systems are modeled. The effects of climate change on electricity consumption, power generation, and power infrastructure are modeled. Second, this paper proposes a coordinated dispatch approach to address the computational burden attributed to the temporal coupling features of energy storage. Thirdly, a capacity credit (CC) assessment framework combining a multi-time-scale dispatch approach of energy storage is developed to model the effect of climate change and communication failures on the capacity credit of renewable energy. Finally, the proposed method is validated by the provincial power system of Guangxi (GX).**

Keywords—Reliability assessment, Capacity credit, Cyber-physical power system, Energy storage, Climate change.

NOMENCLATURE

Indices and Sets

d	Index of natural day periods from 1 to D.
h	Index of hourly periods from 1 to H.

Parameters

C^{res}	Capacity of renewable resource including solar and wind.
λ_g / λ_u	Temperature-induced de-rating factors of coal plant unit g / nuclear unit u.
$T_{g,\max}$ / $T_{u,\max}$	Reference temperature for 100% output of coal plant unit g / nuclear unit u.
C_g / C_u	Capacity of coal plant unit g / nuclear unit u
$T_{tr,\max}$	Maximum temperature of conductor tr.
T_{ave}	Average heat transfer coefficient of transmission line.
ϕ	Conductor diameter of transmission line.
ε	Emissivity of conductor surface.
σ	Stefan-Boltzmann constant.
δ	Solar flux.
α	Solar absorptivity of conductor surface.
R	AC resistance of conductor.
I	Electric current of transmission line.
U	Conductor voltages.
θ	Power factor.
C_l	Rated transmission capacity of transmission line l.
λ_l	De-rating factors of transmission line l.

Variables

P_t^{ava}	Total available capacity at time t.
P_t^{res}	Total power generation of renewable resource at time t.
P_t^{tr}	Total transmission power of the transmission line at time t.
P_t^{h}	Total power generation of hydro at time t.
P_t^{ES}	Total power output of energy storage at time t.
$P_{e,t}^{\text{cha}}$ / $P_{e,t}^{\text{dis}}$	Changing/discharging power of energy storage e at time t.
L_t	Load demand at time t.
P_t^{loss}	Load curtailment at time t.
S_t^{system}	The state of system at time t.
T_t	The air temperature at time t.

I. INTRODUCTION

A. Background and Motivation

The Cyber-Physical Power System (CPPS), integrating power and communication systems, is central to modern power infrastructure. Communication systems are critical for

This work was supported in part by the Specific Research Project of Guangxi for Research Bases and Talents (2022AC21257).

monitoring, control, and protection, but their failures can cause delays, data loss, or control failures, potentially triggering cascading outages. Meanwhile, the shift to low-carbon energy through renewable sources like wind and solar is vital for sustainability, yet their intermittency challenges power system adequacy. Climate-driven variability exacerbates these challenges. Thus, this paper explores the impacts of climate change and communication failures on grids and advances methods for efficient power system adequacy assessment.

B. Literature Review

For assessing power system adequacy within the context of highly integrated cyber-physical systems, Ref. [1], [2] examined the direct and indirect impact of communication systems on power systems. On this basis, an approach based on a ternary Markovian model that considers cyber-physical component interactions was proposed [3]. Ref. [4] analyzes and predicts cybersecurity breaches and explores the impact of cyberattacks and physical component damage on CPPS.

To realize refined capacity credit assessment, a multi-time-scale CC assessment framework is proposed, considering daily fluctuations induced by extreme weather and demand response [5]. Ref. [6] studied the impacts of wind speed, solar radiation, and load variation on CC. However, climate-induced temperature increase has an effect on both the load demand and the energy supply systems, which then leads to a drop in power system reliability [7].

Energy storage is a promising solution to address the uncertain output power of renewable energy sources (RES) [5], [8]. However, the dispatch of pumped hydro storage (PHS) and battery energy storage (BES) is hindered by the coupling of different timescales, resulting in numerous variables and increased computational complexity [9].

To sum up, there are three gaps that remain to be improved: (1) The impact of communication system failures should be considered in capacity credit assessment. (2) There is a lack of research integrating the impacts of temperature increases resulting from climate change with reliable capacity evaluations. (3) Computational complexity induced by the coupling of BES and PHS should be addressed.

To address the issues, a capacity credit assessment framework is developed that combines a multi-time-scale dispatch approach for energy storage while considering the impacts of climate change and communication system failures. The main contributions of this paper are summarized as follows:

1) A capacity credit assessment framework combining the uncertainties of renewable sources and load is developed to model the effect of climate change and communication system failures on the capacity credit of RES.
2) This paper introduces a two-stage optimizing method based on seasonal trend decomposition to address the computational burden attributed to the temporal coupling features of energy storage. In the first stage, seasonal fluctuations are smoothed by PHS, and the daily SOC of PHS is obtained, serving as the benchmark for the operation of PHS in the subsequent phase. In the second stage, PHS is integrated with BES to facilitate the smoothing of the annual net load curve on an hourly time scale.

The paper is organized as follows: Section II introduces the methodology of capacity credit evaluation; Section III describes the EES and PHS coordinated dispatching approach; Section IV presents case study results; and Section V provides conclusions.

II. Framework and Methodology

A. Reliability Evaluation

The reliability evaluation method based on sequential Monte Carlo Simulation (SMCS) mainly includes three steps: state generation, state analysis, and reliability indices calculation [10].

Reliability indices calculation: load loss probability (LOLP) and expected power not supplied (EENS) indices are used to evaluate the reliability of electrical power systems. LOLP and EENS are calculated by Eq. (1) and (2), respectively. The system's status is determined at each moment based on the load curtailment, as shown in Eq. (3).

$$LOLP = \frac{1}{M \cdot T} \sum_{m=1}^{M} \sum_{t=1}^{T} S_t^{\text{system}} \tag{1}$$

$$EENS = \frac{1}{M} \sum_{m=1}^{M} \sum_{t=1}^{T} P_t^{loss} \tag{2}$$

$$S_t^{\text{system}} = \begin{cases} 1, if\ P_t^{loss} > 0 \\ 0, otherwise \end{cases} \tag{3}$$

B. Capacity Credit Evaluation

Capacity credit evaluation for RES, including wind and solar, in this paper is based on the equivalent firm capacity (EFC) [11]. The original system is composed of coal plants, nuclear, hydro, transmission lines, and renewable energy sources (solar and wind). The new system introduces the concept of a benchmark unit to replace renewable energy. The output of the benchmark unit is modified by the dichotomization method, ensuring that the reliability level of the new system aligns with that of the original system. The credit capacity of renewable energy can be obtained when the convergence accuracy meets the established criteria. The CC evaluation method is formulated as follows:

$$\begin{aligned} &R\left\{P^{\text{ava}} + P^{\text{tr}} + P^{\text{h}} + P^{\text{ES}} + P^{\text{res}}, L\right\} \\ &= R\left\{P^{\text{ava}} + P^{\text{tr}} + P^{\text{h}} + P^{\text{ES}} + P^{\text{EFC}}, L\right\} \end{aligned} \tag{4}$$

where, $R\{X, L\}$ is the function of reliability index, such as EENS. X is the set of the existing units in the system. L is the load demand. P^{EFC} is the benchmark unit that realizes the same reliability level as that with renewable.

The credible capacity of RES is calculated as follows:

$$CC = \frac{P^{\mathrm{EFC}}}{C^{\mathrm{res}}} \tag{5}$$

C. Quantifying The Impacts of Climate Change

Climate change affects generation resource adequacy deeply by influencing electricity consumption, generation, and electricity supply infrastructure. Regarding the impact of climate change on electricity consumption, the response functions of electricity consumption to climate change exhibit asymmetric U-shaped curves [12].

Regarding the impact of climate change on electricity generation, the atmospheric variables resulting from climate change can impact the efficiency of photovoltaic power generation [13].

Regarding the impact of climate change on electricity supply infrastructure, the temperature increases induced by climate change affect the cooling water usage of thermal and nuclear generators. The impacts are defined as the capacity at risk of outage [14]. The formulations are as follows:

$$C_{\mathrm{t}}^{\mathrm{out,g}} = \begin{cases} \lambda_g C_g \left(T_t - T_{g,\max}\right), T \geq T_{g,\max} \\ 0, \qquad\qquad T < T_{g,\max} \end{cases} \tag{6}$$

$$C_{\mathrm{t}}^{\mathrm{out,u}} = \begin{cases} \lambda_u C_u \left(T_t - T_{u,\max}\right), T \geq T_{u,\max} \\ 0, \qquad\qquad T < T_{u,\max} \end{cases} \tag{7}$$

where Eq. (6) and (7) represents the outage capacity of thermal and nuclear, respectively.

Regarding the impact of climate change on transmission lines, it can be quantified by assessing their respective carrying capacities [14]. The formulations are as follows:

$$I = \sqrt{\frac{\pi T_{\mathrm{ave}} \phi \left[T_{tr,\max} - T_t\right] + \pi\varepsilon\sigma\phi\left[T_{tr,\max}^4 - T_t^4\right] - \delta\phi\alpha}{R}} \tag{8}$$

$$C_{l,t}^{\mathrm{out}} = \lambda_l \left(C_l - \sqrt{3} \cdot \theta \cdot I \cdot U\right) \tag{9}$$

where, Eq. (8) represents the transmitted electricity current. Eq. (9) represents the outage capacity of high-voltage transmission lines.

III. Model Formulation of Dispatch

A. Coordinated Dispatch Approach for BES and PHS

Fig. 1 shows the flowchart of the BES and PHS coordinating dispatch approach, which involves two-stage optimization. In the first stage, the seasonal component represents the periodic variation, and the trend component can be regarded as the long-term trend [9]. Since PHS is a long-term, high-capacity energy storage, these fluctuations are smoothed by pumped hydro storage on the daily time scale. The daily SOC of pumped hydro storage was obtained, serving as the benchmark for the operation of pumped hydro storage in the subsequent phase. In the second stage, PHS is integrated with BES to facilitate the smoothing of the annual net load curve on the hourly time scale.

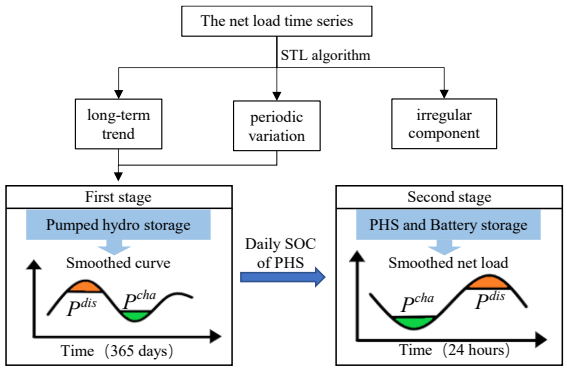

Fig. 1. Battery storage and PHS coordinating dispatch approach.

Once the communication system simulation and the unit's operational state are finished, the effects of climate change are measured using the equations from Part C of Chapter II. This allows for the calculation of the net load curve, which takes into account both the communication system's failure and the influence of climate change. The resulting net load curve is then utilized for scheduling energy storage.

B. Mathematical Formulation

The net load time series is decomposed into three components, including trend, seasonal, and irregular components, by the STL algorithm:

$$\begin{cases} L^{\mathrm{net}} = L - P^{\mathrm{res}} - P^{\mathrm{tr}} - P^{\mathrm{h}} \\ L^{\mathrm{net}} = L^{\mathrm{LT}} + L^{\mathrm{ST}} + L^{\mathrm{R}} \end{cases} \tag{10}$$

where, L^{LT} is the trend component. L^{ST} is the seasonal component. L^{R} is the irregular component.

In the first stage, to minimize the seasonal fluctuations, the objective function and operation constraints are defined as follows:

1) Objective Function:

$$\min \sum_{d=1}^{\mathrm{D}} (L_d^{\mathrm{mh}})^2 \tag{11}$$

$$L_d^{\mathrm{mh}} = L_d^{\mathrm{LT}} + L_d^{\mathrm{ST}} + P_d^{\mathrm{phs,cha}} - P_d^{\mathrm{phs,dis}}, \forall d \tag{12}$$

where the sum of squares is a proposed indicator for evaluating curve volatility in Eq. (11). L_d^{mh} is the smoothed long-term load on the daily time scale. $P_d^{\mathrm{phs,cha}}$, $P_d^{\mathrm{phs,dis}}$ are the charging power, and the discharging power of PHS on the daily time scale, respectively.

2) Daily Operation Constraints:

$$E_d^{\mathrm{phs}} = E_{d-1}^{\mathrm{phs}} + k_{\mathrm{phs,c}} P_d^{\mathrm{phs,cha}} - \frac{P_d^{\mathrm{phs,dis}}}{k_{\mathrm{phs,d}}}, \forall d \tag{13}$$

$$e_{\min} E_{\max}^{\mathrm{phs}} \leq E_d^{\mathrm{phs}} \leq e_{\max} E_{\max}^{\mathrm{phs}}, \forall d \tag{14}$$

$$0 \leq P_d^{\mathrm{phs,cha}} \leq P_{\max}^{\mathrm{phs}} u_d^{\mathrm{phs}}, \forall d \tag{15}$$

$$0 \leq P_d^{\mathrm{phs,dis}} \leq P_{\max}^{\mathrm{phs}} \left(1 - u_d^{\mathrm{phs}}\right), \forall d \tag{16}$$

$$E_0^{\mathrm{phs}} = E_{\mathrm{D}}^{\mathrm{phs}} \tag{17}$$

where E_d^{phs} is PHS energy level on day d. $k_{\mathrm{phs,c}}$, $k_{\mathrm{phs,d}}$ are the

charging and discharging efficiency, respectively. $e_{\max}$, $e_{\min}$ are the ratio of upper and lower energy storage capacity. u_d^{phs} is the auxiliary binary variable to ensure there is only one operational state for PHS. Eq. (13) represents the transition of SOC between two adjacent days. The energy and power constraints of PHS as listed as Eq. (14) -(16), respectively. Eq. (17) imposes the same SOC at the beginning and at the end of the year for multi-year operation. The daily SOC obtained in the first stage serves as a constraint to limit the daily energy change of PHS in the second stage.

In the second stage, to smooth the annual net load, the objective function and operation constraints are defined as follows:

1) Objective Function:

$$\min \sum_{h=1}^{\mathrm{H}} (L_h^{me})^2 \tag{18}$$

$$L_h^{\text{me}} = L_h^{\text{net}} + P_h^{\text{phs,cha}} - P_h^{\text{phs,dis}} + P_h^{\text{bes,cha}} - P_h^{\text{bes,dis}}, \forall h \tag{19}$$

where, L_h^{me} is the smoothed net load on the hourly time scale. $P_d^{\text{bes,cha}}$, $P_d^{\text{bes,dis}}$ are the charging power, and the discharging power of BES on the hourly time scale, respectively. $P_d^{\text{phs,cha}}$, $P_d^{\text{phs,dis}}$ are the charging power, and the discharging power of PHS on the hourly time scale, respectively.

2) Hourly Operation Constraints:

$$E_h^{\text{bes}} = E_{h-1}^{\text{bes}} + k_{\text{bes,c}} P_h^{\text{bes,cha}} - \frac{P_h^{\text{bes,dis}}}{k_{\text{bes,d}}}, \forall h \tag{20}$$

$$e_{\min} E_{\max}^{\text{bes}} \le E_h^{\text{bes}} \le e_{\max} E_{\max}^{\text{bes}}, \forall h \tag{21}$$

$$0 \le P_h^{\text{bes,cha}} \le P_{\max}^{\text{bes}} u_h^{\text{bes}}, \forall h \tag{22}$$

$$0 \le P_h^{\text{bes,dis}} \le P_{\max}^{\text{bes}} \left(1 - u_h^{\text{bes}}\right), \forall h \tag{23}$$

$$E_0^{\text{bes}} = E_{\text{H}}^{\text{bes}} \tag{24}$$

$$\sum_{h=1}^{\mathrm{H}} \left(P_h^{\text{phs,cha}} - P_h^{\text{phs,dis}}\right) = P_d^{\text{phs,cha}} - P_d^{\text{phs,dis}}, \mathrm{H} \propto d \tag{25}$$

$$E_{\text{H}}^{\text{phs}} = E_d^{\text{phs}}, \mathrm{H} \propto d \tag{26}$$

where $E_{\text{H}}^{\text{phs}}$ is PHS energy level on the last hour of the day. Eq. (20)-(24) represents the constraints of battery energy storage. The equations annotations are comparable to Eq. (13)-(17). Eq. (25)-(26) represents the cumulative charge and discharge within a 24-hour period of PHS should correspond to the optimization outcomes derived from the first stage. The additional daily constraints of PHS are comparable to Eq. (20)-(24).

IV. Case Study

A. Data Description

1) Consumption and Installed Capacity

The case study is based on the power system of Guangxi in 2022 [15], [16]. The generator information comes from China Electricity Statistical Yearbook 2022, as shown in table I.

TABLE I. TOTAL INSTALLED CAPACITY BY GENERATION TECHNOLOGY OF GX IN 2022

Installed capacity (GW)				
Coal	***Nuclear***	***Hydro***	***Wind***	***Solar***
26.79	2.17	18.72	11.86	5.20

2) Reliability Parameters

The reliability parameters of generation technologies and transmission lines are collected from the National Electric Reliability Annual Report 2022. The reliability parameters of units by generation technology include capacity, Mean Time to Failure (MTTF), Mean Time to Repair (MTTR), and forced outage rate (FOR). The reliability parameters of transmission lines include transmission capacity, voltage, Mean Time to Failure (MTTF), Mean Time to Repair (MTTR), and forced outage rate (FOR). Table II shows the reliability parameters of communication systems.

TABLE II. RELIABILITY PARAMETERS OF INFORMATION COMPONENTS

Items	***MTTR (h)***	***MTTF (h)***	***FOR (%)***
Switch	48	28000	0.17
Communication management unit	48	125000	0.0038

3) Scenario Descriptions

This paper sets eight scenarios to verify the effectiveness of the proposed methods, as shown in Table III. The baseline scenario (BAU) is considered that the communication system is completely reliable and does not take into account the impact of climate change and the role of energy storage. S1, S2, and S3 consider the effects of communication system failures, climate change, and energy storage, respectively. S4, S5, S6, and S7 consider the combinations of information system failures, climate change, and energy storage, respectively.

TABLE III. SCENARIO DESCRIPTIONS

Scenarios	***Communication system failures***	***Climate change***	***Energy storage***
BAU	-	-	-
S1	√	-	-
S2[a]	-	√	-
S3	-	-	√
S4[a]	√	√	-
S5	√	-	√
S6[a]	-	√	√
S7[a]	√	√	√

[a.] The average temperature in these scenarios is assumed to increase by 0.15°C compared with the BAU scenario.

B. Result

1) Power System Adequacy Assessment Results of Eight Scenarios

Table IV shows the power system adequacy assessment results of the eight scenarios. Comparisons of the results of BAU and S1 show that EENS increases from 11.78 GWh to 13.31

GWh, and LOLP increases by only 0.01%. After considering the impact of communication system failures, the reliability of the power system will decrease. However, the probability of system outage does not increase significantly. The reason is that the FOR of information components is low, and the communication system has an indirect effect on the power system.

Compared with the reliability indexes between the BAU and S2, the results show that the reliability of the Guangxi power grid is sensitive to climate changes. From the results of S4, it can be seen that communication system failures exacerbate the severity of power outages when the effects of climate change are considered. The EENS in BAU is 11.78 GWh, decreasing to 4.63 GWh in S3. The LOLP decreases from 0.18% to 0.09%. This is because energy storage could reduce the probability of power system outage by absorbing excess wind and solar to store electricity and then discharging it at peak demand. S5, S6, and S7 results show that energy storage can reduce the amount of system loss of load and improve system reliability

In terms of capacity credit of wind and solar, the CC exhibits a decline, from 12.76% in BAU to 12.71%. The reason is that communication system failures can disrupt the normal operation of wind and photovoltaic units, resulting in a decrease in their equivalent credible capacity. A comparison of the results of BAU and S2 shows that credible capacity decreases from 2.18 GW to 1.96 GW and CC decreases from 12.76% to 11.51%. The reason is that the increase in temperature caused by climate change affect the efficiency of solar, resulting in a decrease in the correlation between the load profile and solar generation. The credible capacity in S4 is 1.97 GW, an increase of 0.51% over the 1.96 GW in S2. This phenomenon can be attributed to a reduction in the output of units because of communication system failures. As a result, the utilization rates of wind and PV energy sources increase.

The results of S3, S5, S6, and S7 show that energy storage plays a significant role in enhancing the adequacy of the power system. Indeed, energy storage is a promising option to improve the generation adequacy of renewables. The CC of renewable energy sources is augmented as a result of the strengthened correlation between renewable generation and load through peak valley regulation.

TABLE IV. POWER SYSTEM ADEQUACY ASSESSMENT RESULTS

Scenarios	*EENS (GWh/y)*	*LOLP (%)*	*Credible capacity (GW)*	*CC (%)*
BAU	11.78	0.18	2.18	12.76
S1	13.31	0.19	2.17	12.71
S2	64.24	0.65	1.96	11.51
S3[b]	4.63	0.09	2.46	14.45
S4	68.52	0.68	1.97	11.55
S5[b]	5.51	0.10	2.44	14.3
S6[b]	38.12	0.44	2.11	12.36
S7[b]	41.28	0.46	2.10	12.35

[b] Scenarios with 300 MW BES and 1000 MW PHS installation, and their durations are set to be 2 h and 6 h, respectively.

2) Comparison of Computational Efficiency for BES and PHS Coordinating Dispatch Approach

PHS is long-term, high-capacity energy storage, which is used to smooth fluctuations on the daily time scale, as shown in Fig. 2 (a). The BES, as a complementary system, smooths the smaller variations on an hourly time scale (Fig. 5 (b)). Table V shows the comparison of different dispatch approaches for BES and PHS. The results show that the two-stage optimal scheduling method is used to improve the calculation rate by 36% compared to the conventional method.

TABLE V. COMPARISON OF DIFFERENT DISPATCHED APPROACH

Approach	*Times (s)*	*LOLP (%)*	*CC (%)*
With two-stage optimization	231	0.091	14.45
Without two-stage optimization	362	0.085	14.98

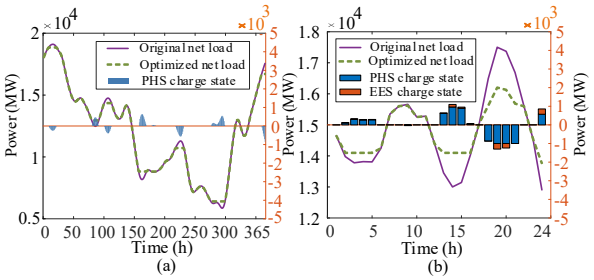

Fig. 2. Optimization results of daily time scale.

V. CONCLUSION

This paper establishes a capacity credit assessment framework considering the effects of communication system failures and climate change on CPPS adequacy. To address the computational burden, a coordinated dispatch approach of multiple storage technologies based on the STL algorithm is proposed. The proposed method and framework are validated by the provincial power system of GX.

REFERENCES

[1] B. Falahati, Y. Fu, and L. Wu, "Reliability Assessment of Smart Grid Considering Direct Cyber-Power Interdependencies," *IEEE Trans. Smart Grid*, vol. 3, no. 3, pp. 1515–1524, Sep. 2012, doi: 10.1109/TSG.2012.2194520.

[2] B. Falahati and Y. Fu, "Reliability Assessment of Smart Grids Considering Indirect Cyber-Power Interdependencies," *IEEE Trans. Smart Grid*, vol. 5, no. 4, pp. 1677–1685, Jul. 2014, doi: 10.1109/TSG.2014.2310742.

[3] P. A. Oyewole and D. Jayaweera, "Power System Security With Cyber-Physical Power System Operation," *IEEE Access*, vol. 8, pp. 179970–179982, 2020, doi: 10.1109/ACCESS.2020.3028222.

[4] A. Rostami, M. Mohammadi, and H. Karimipour, "Reliability assessment of cyber-physical power systems considering the impact of predicted cyber vulnerabilities," *Int. J. Electr. Power Energy Syst.*, vol. 147, p. 108892, May 2023, doi: 10.1016/j.ijepes.2022.108892.

[5] R. Wang, S. Wang, G. Geng, and Q. Jiang, "Multi-time-scale capacity credit assessment of renewable and energy storage considering complex operational time series," *Appl. Energy*, vol. 355, p. 122382, Feb. 2024, doi: 10.1016/j.apenergy.2023.122382.

[6] S. Muaddi and C. Singh, "Investigating capacity credit sensitivity to reliability metrics and computational methodologies," *Appl. Energy*, vol. 325, p. 119825, Nov. 2022, doi: 10.1016/j.apenergy.2022.119825.

[7] A. T. D. Perera, V. M. Nik, D. Chen, J.-L. Scartezzini, and T. Hong, "Quantifying the impacts of climate change and extreme climate events on energy systems," *Nat. Energy*, vol. 5, no. 2, pp. 150–159, Feb. 2020, doi: 10.1038/s41560-020-0558-0.

[8] B. Wang *et al.*, "A four-stage fast reliability assessment framework for renewables-dominated strong power systems with large-scale energy storage by temporal decoupling and contingencies filtering," *Appl. Energy*, vol. 362, p. 123035, May 2024, doi: 10.1016/j.apenergy.2024.123035.

[9] S. Jiang, S. Wen, M. Zhu, Y. Huang, and H. Ye, "Scenario-Transformation-Based Optimal Sizing of Hybrid Hydrogen-Battery Storage for Multi-Timescale Islanded Microgrids," *IEEE Trans. Sustain. Energy*, vol. 14, no. 3, pp. 1784–1795, Jul. 2023, doi: 10.1109/TSTE.2023.3246592.

[10] X. He *et al.*, "A robust reliability evaluation model with sequential acceleration method for power systems considering renewable energy temporal-spatial correlation," *Appl. Energy*, vol. 340, p. 120996, Jun. 2023, doi: 10.1016/j.apenergy.2023.120996.

[11] S. Nolan, M. O'Malley, M. Hummon, S. Kiliccote, and O. Ma, "A methodology for estimating the capacity value of demand response," in *2014 IEEE PES General Meeting | Conference & Exposition*, Jul. 2014, pp. 1–5. doi: 10.1109/PESGM.2014.6939174.

[12] L. Wenz, A. Levermann, and M. Auffhammer, "North–south polarization of European electricity consumption under future warming," *Proc. Natl. Acad. Sci.*, vol. 114, no. 38, pp. E7910–E7918, Sep. 2017, doi: 10.1073/pnas.1704339114.

[13] S. Jerez *et al.*, "The impact of climate change on photovoltaic power generation in Europe," *Nat. Commun.*, vol. 6, no. 1, p. 10014, Dec. 2015, doi: 10.1038/ncomms10014.

[14] H. Chen *et al.*, "Estimating the impacts of climate change on electricity supply infrastructure: A case study of China," *Energy Policy*, vol. 150, p. 112119, Mar. 2021, doi: 10.1016/j.enpol.2020.112119.

[15] B. Li, M. Chen, H. Zhong, D. M. Kammen, and X. Li, "Open-Source Chinese Power System with High Spatial and Temporal Resolution," in *2022 5th International Conference on Energy, Electrical and Power Engineering (CEEPE)*, Apr. 2022, pp. 315–321. doi: 10.1109/CEEPE55110.2022.9783435.

[16] B. Li and G. Wei, "Two-Stage Synthetic Power System Modelling Based on Transmission Expansion Planning," in *2024 IEEE Power & Energy Society General Meeting (PESGM)*, Jul. 2024, pp. 1–5. doi: 10.1109/PESGM51994.2024.10688387.